4. PARTICIPATION IN THE ASDEX UPGRADE PROGRAMME

M.E. Manso and F. Serra (Heads), L. Cupido, S. Hacquin, I. Nunes, T. Ribeiro, J. Santos,
A. Silva, F. Silva, P. Varela, S. Vergamota

4.1. INTRODUCTION

The Portuguese participation in the ASDEX Upgrade programme has been mainly focussed on the following areas:

- Microwave reflectometry;
- MHD and Turbulence.

4.2. MICROWAVE REFLECTOMETRY

4.2.1. Introduction

This project has had the following main objectives:

- Routine operation and maintenance of both the fixed frequency channels, which monitor the density fluctuations, and the ultra fast sweeping system that measures the density profiles at both the low and high magnetic field sides;
- Upgrades and new channels of the reflectometry diagnostic;
- Upgrades of the dedicated control and data acquisition system;
- Studies for diagnostic exploitation;
- New applications relevant for ITER;
- Modeling of reflectometry experiments;
- Plasma physics studies.

4.2.2. Upgrades and new channels of the reflectometry diagnostics

4.2.2.1. Main activities

The following main activities were carried out:

- Development of in-phase and quadrature heterodyne detection for the V-band fixed frequency channel using synthesizer sources, to study radial correlation parameters of plasma turbulence;
- Development of a numerical code to calculate the calibrated amplitude and phase signals from I and Q signals;
- Improvements in the heterodyne detections of the V and W-band channels in order to increase the S/N ratio;
- Development of switches to commute between fixed frequency and broadband operation compatible with the stray magnetic field environment, to be installed in the diagnostic section located at the torus hall;
- Installation of a new harmonic mixer and active frequency doubler in the Q-band channel (LFS), to replace the old equipment with degraded performance due to aging;
- Assessment of possible locations for the W-band antenna (X mode) at the LFS that may have to be displaced due to the installation of the upgraded ICRH system.

4.2.2.2. Fluctuations monitor

The heterodyne detection for the V-band fixed frequency channel is equipped with full frequency synthesizers designed and constructed at CFN, used for both the main and local oscillators. This solution overcomes the poor phase noise performance of the broadband oscillators utilized in all the reflectometry channels of the ASDEX Upgrade diagnostic. This development has the particularity of synthesizing the frequency by phase locking a broadband microwave source in excess of one octave tuning range. Also, this scheme is capable of fast frequency switching which permits to change the operating frequency by several GHz in less than 1ms. Figure 4.1 shows the current configuration of the V-band fixed frequency channel. The use of a heterodyne phase and quadrature detection implies the calibration of the system before any quantitative analysis can be performed. Ideally the system should deliver two signals with the same amplitude, no offsets and a phase difference of exactly 90º between them, namely a sine and a cosine:

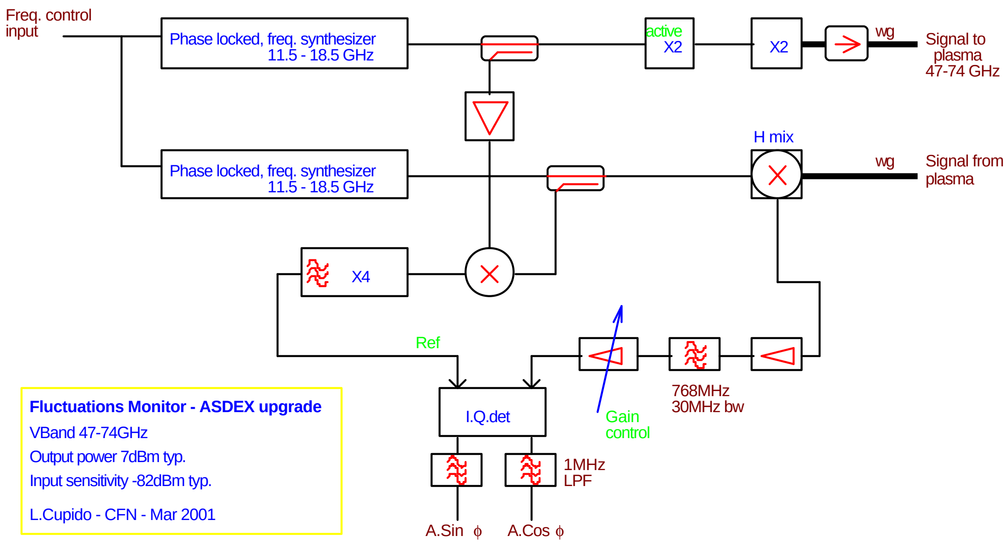

Figure 4.1 - Schematic configuration of the V band heterodyne reflectometer to monitor plasma fluctuations on ASDEX Upgrade

$$Q = A\sin(q) \tag{4.1}$$

$$I = A\sin(q + 90^{o}) = A\cos(q) \tag{4.2}$$

In fact two signals are defined as:

$$Q = A\sin(q) + Q_0 \tag{4.3}$$

$$I = A \cdot A_{IQ} \sin(q + F) + I_0 \tag{4.4}$$

where I_0 and Q_0 are the offsets of the phase and quadrature signals, respectively, and A_{IQ} and $F = (90^{o} + W)$, being Ω the quadrature error, are the amplitude and phase imbalances between them. For the case of the V-band fluctuations monitor channel, $A_{IQ} = 1$ and $W = 0$ were assumed. The calibrated signals can then be written as:

$$A\sin(q) = Q - Q_0 \tag{4.5}$$

$$A\cos(q) = I - I_0 \tag{4.6}$$

After straightforward manipulations the expressions for the amplitude and phase signals were obtained:

$$\begin{aligned} A &= \sqrt{A^2\sin^2(q) + A^2\cos^2(q)} \\ &= \sqrt{(Q - Q_0)^2 + (I - I_0)^2} \end{aligned} \tag{4.7}$$

$$q = \arctan\left(\frac{A\sin(q)}{A\cos(q)}\right) = \arctan\left(\frac{Q - Q_0}{I - I_0}\right) \tag{4.8}$$

A calibration of the V-band fluctuations monitor channel was performed using several test shotfiles acquired for that purpose. Each one used a different probing frequency in a way that the available range in frequency for this channel was covered. To perform the data analysis two computer codes were developed. One for extraction of the calibration factors (offsets) from the test shotfiles and another one to extract the amplitude and phase signals from the I and Q components, using the measured offsets.

The first one reads the test shotfiles and extracts the offsets for its "in phase" (I) and "in quadrature" (Q) components. As these signals are stationary, this is done by calculating their mean average value. The code also calculates the mean standard deviation for each of them, which is a measure of the data dispersion and provides a good estimate for the error of the extracted offsets. Figure 4.2 shows an example for a typical test.

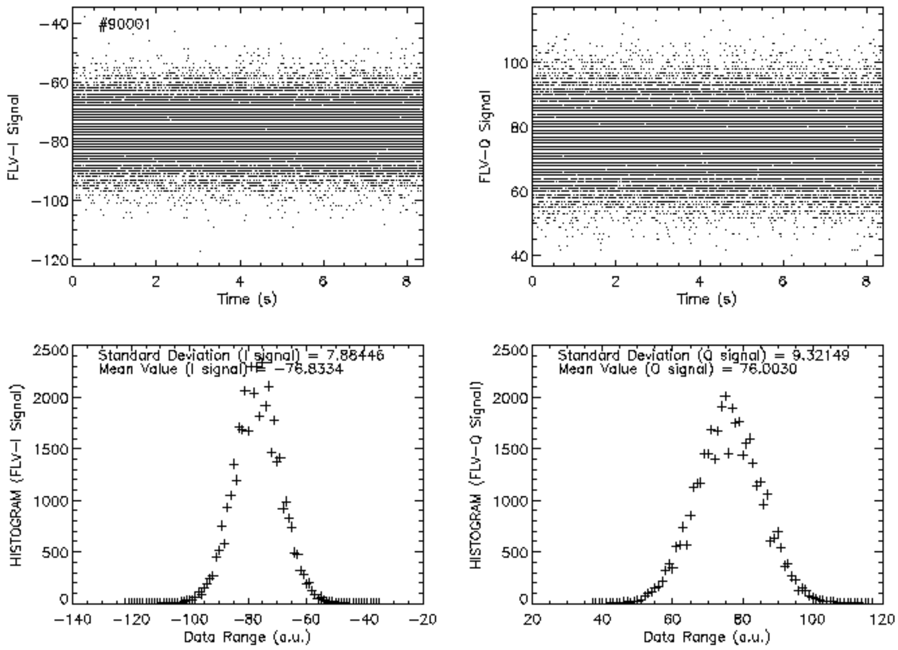

Figure 4.2 – Raw data signals for the components I (a) and Q (b) for the test shotfile #90001 acquired with the vessel opened and used a probing frequency of 72 GHz. The plots (c) and (d) show the respective histograms and also the values for the mean value (offset) and the mean square value (error).

Figure 4.3 presents the offsets for all the test shots made (I and Q), with the associated error bars given by the mean standard deviation. All the test data from which this plot was obtained were acquired with the vessel opened, and with practically no temporal interval between them. All of them were made with an absorber inside the vessel, except one of them, for which the absorber was taken out. The offsets stay fairly constant suggesting its constancy for the whole probing frequency domain available for this channel. The error is of the order of 10%.

More tests were performed later, for some of the previous probing frequencies, now with vacuum (vessel sealed) and no plasma. Significant variations in the calibration factors were observed (Figure 4.4 in comparison to Figure 4.2). Since there was a bigger temporal delay between them (~1 hour), and between them and the previous set (~days), this suggests a dependence on the conditions of the acquisition, for instance the temperature, which varied between acquisitions.

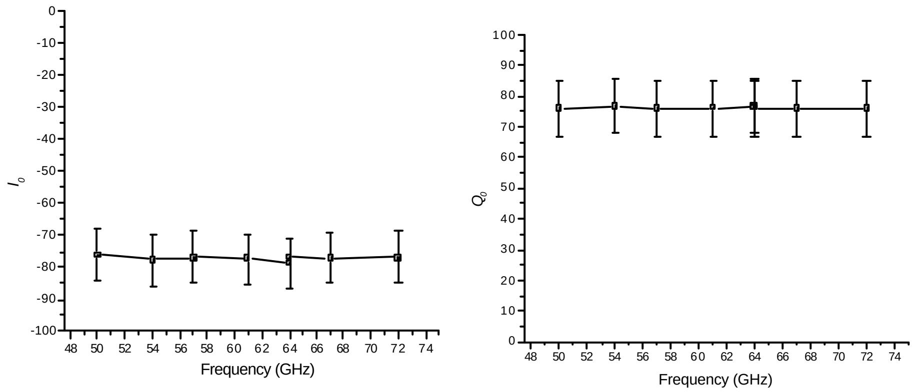

Figure 4.3 – I and Q offsets and its error bars vs. the probing frequencies of the test shotfiles made, showing constancy for the whole domain.

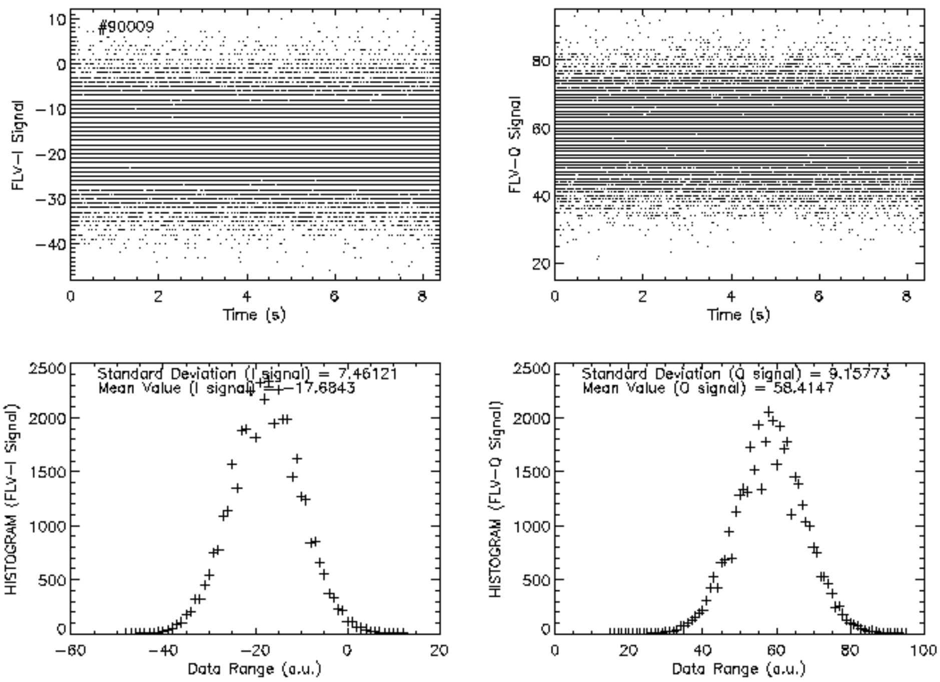

Figure 4.4 – Raw data signals for the components I (a) and Q (b) for the test shotfile #90009 acquired with the vessel sealed and no plasma inside using a probing frequency of 64 GHz. The plots (c) and (d) show the respective histograms and also the values for the mean value (offset) and the mean square value (error).

The second code mentioned was developed to look at the corresponding signals for public shots. This code reads the I and Q components (raw data) and uses the measured offsets to calculate the calibrated amplitude and phase signals. It also calculates their histogram as this is a good tool for a preliminary data characterisation. The code was used on some shotfiles acquired during last experimental campaign using different I and Q offsets. For discharge #14540, results are shown with the offsets given by the average offset value of the first test set of Figure 4.3 (Figure 4.5). Plotting the correspondent histograms the sensitivity of the amplitude and phase data to the calibration factors can be checked.

The observed temporal variability of the calibration factors, stress that this subject must be further studied in order to achieve a good procedure for the calibration of the experimental data. Also possibly a calibration on an every-day basis, or even in a shot-to-shot basis might have to be done.

4.2.3. Upgrades of the dedicated control and data acquisition system

The following main tasks were performed:

- Upgrade of the 250 MHz data acquisition VME boards for larger memory (3 MBytes), which permits to increase the number of measured profiles per discharge from 720 to 3066;
- Integration of a new timing/acquisition clock generation board and development of the required software;
- Modification of the device drivers for the upgrade graphical user interface;
- Development of hardware and software to split the reflectometry diagnostic into two separate diagnostics: one for fixed frequency operation, the other for broadband sweeping.
- Implementation of software to control the new fixed frequency V-band heterodyne channel;
- Development of a Web supported data base with information on data acquisition and operating modes of the reflectometry diagnostic and relevant data from other diagnostics for each plasma discharge.

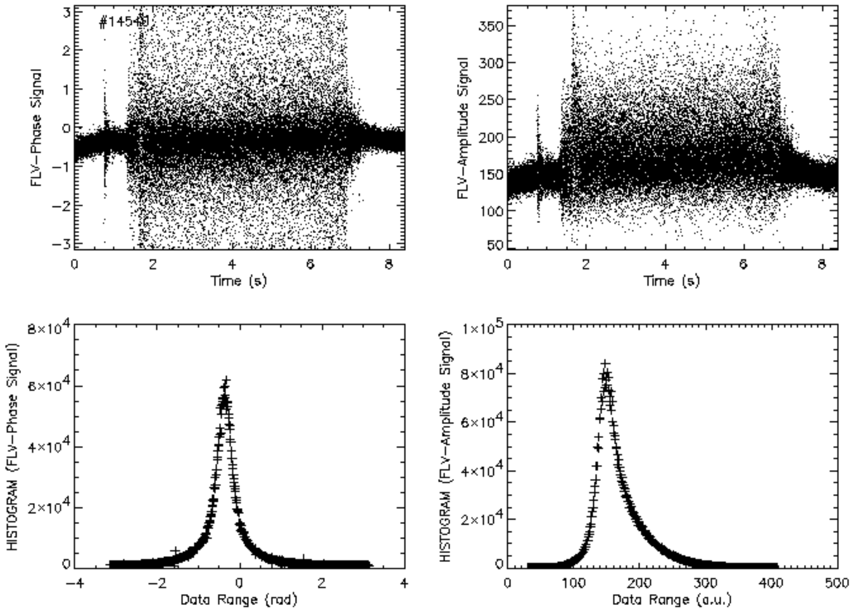

Figure 4.5 – Calibrated amplitude and phase signals and corresponding histograms.

4.2.4. Studies for diagnostic exploitation

4.2.4.1. Main activities

The following main activities were made:

- Comparison of two data processing tools developed for automatic profile evaluation: single sweep and burst-mode analysis;
- Development of software tools to generate automatically level 2 shot files in the ASDEX Upgrade shotfile system containing the results of the burst-mode analysis (in final phase of implementation);
- Development of novel algorithms for classifying the density profiles with a parameter that weights the degree of distortion due to the plasma turbulence, enabling automatic profile averaging and selection (in progress);
- Development of software tools to detect automatically the edge pedestal parameters (density, position, and width) with high spatial and temporal resolutions;
- Absolute calibration of density profiles using both O and X mode reflectometry;
- Development of algorithms to extract information about plasma fluctuations from broadband signals.

4.2.4.2. Automatic pedestal detection

Figure 4.6 shows the time resolved power spectrum of a broadband reflectometry signal and a schematic representation of the method used to detect the edge pedestal. A linear fitting is performed to the group delay curve (white line), in the fixed frequency range 18 – 35 GHz and a second fitting is applied to the range starting at the frequency above which the group delay deviates from the previous linear fitting more than a pre-defined value, and the last measured frequency. The pedestal density is given by

$$n_{ep} \cong f^2/81,$$

with f corresponding to the frequency where the fitting lines intersect.

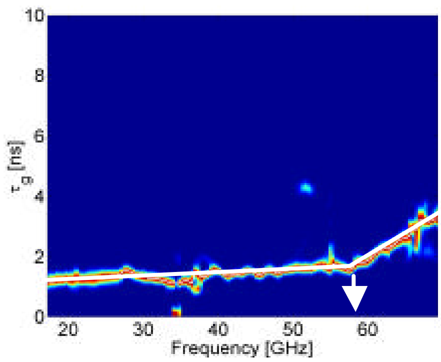

Fig. 4.6 - Schematic representation of the automatic detection of the pedestal density.

4.2.4.3. Absolute calibration of density profiles using both O and X mode reflectometry

The FM-CW reflectometer of ASDEX Upgrade has five channels in O mode and two in X mode at the low field side (LFS). The density range covered by the O mode is $0.3\text{-}15\times10^{19}$ m^{-3}, while for X mode it is determined by the magnetic field.

The quality of the X-mode profiles is very sensitive to the accurate detection of the first reflected frequency. As the detected signal does not provide phase and amplitude separately an amplitude criteria cannot be implemented. An alternative approach has been developed, which is based on the evolution of the reflected signal power. Figure 4.7 shows two raw data signals with and without plasma and the corresponding signal power curves are displayed in Figure 4.8. From the increase of the detected power it is possible to detect where the first reflection occurred.

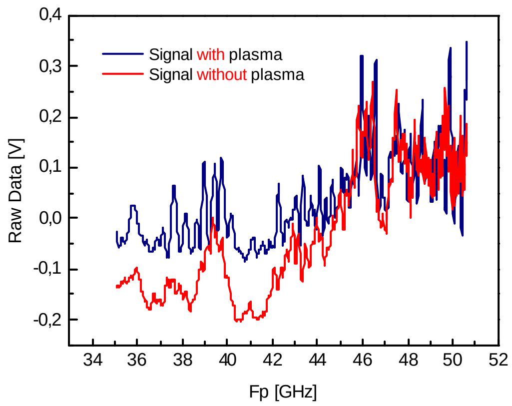

Figure 4.7 – Raw data of two signals of the Q_x band from the same shot with and without plasma.

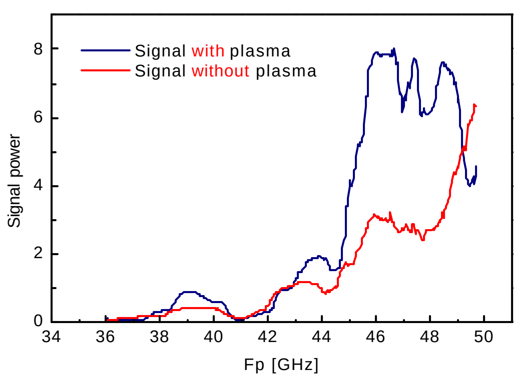

Figure 4.8 – Signal power from the two signals showed in Figure 4.7 with and without plasma.

In cases where this increase is not pronounced, the first fringe cannot be taken from the signal power and some assumptions have to be made. As at zero density the first reflected frequency matches the electron cyclotron frequency (f_{ce}), assuming that no plasma exists behind the antenna (antenna position = 2.374 m), a minor value for the first reflected frequency is found. To major the interval where the first reflected frequency should lie, an estimated value that is routinely used by reflectometry to do profile inversion at ASDEX Upgrade is imposed (R = 2.215 m).

These values impose two boundaries for the first reflected frequency, as shown in Figure 4.9, where the lower curve (green) corresponds to R.=.2.374 m and the upper curve (blue) to R = 2.215 m. When the difference between the signal power curves with and without plasma is very small the gradient can also be used to determine the first reflected frequency. The high sensitivity of the density profiles to errors in the detection of the first reflected frequency can be seen in Figure 4.10.

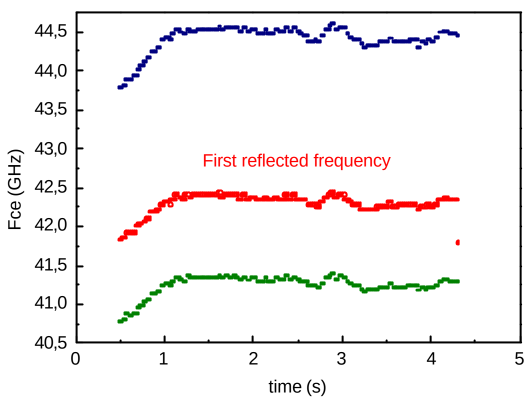

Figure 4.9 – The lower and upper curves correspond to the boundaries that defines the interval where the first reflected frequency must be in (middle curve).

Figure 4.11 shows two density profiles obtained using information from O and X mode measurements. The different bands used at the ASDEX Upgrade reflectometer can also be seen. In this case, the magnetic field is 2.083 T. In order to match the information from O and X modes a multi step procedure was implemented. First the group delay from X mode is obtained using the spectrogram; secondly a numerical algorithm is applied using the magnetic field information to calculate the edge profile. After, the group delay

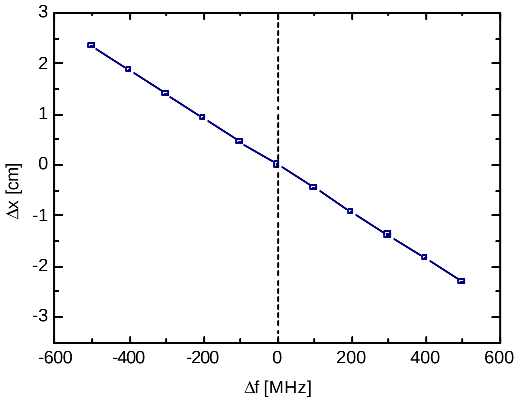

Figure 4.10 – Errors in the positioning of the density profile due to an error in the first reflected frequency.

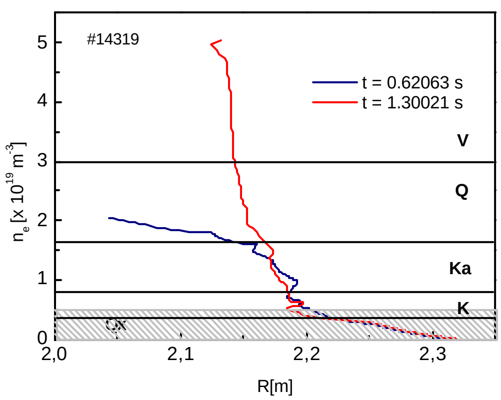

Figure 4.11 – Reconstructed density profiles using X mode data for the initialisation (Q_x band).

curve due to O-mode propagation in the edge profile (measured with X mode) is obtained numerically and fitted with the O mode group delay data, as shown in Figure 4.12, to give a unique group delay. This allow us to obtain the combined O/X mode profiles shown in Figure 4.13.

When X mode is not available an initialisation procedure is used to obtain the group delay curve below the first O-mode probing frequency. The errors due to the initialization are shown in Figure 4.13. Although the errors decrease with increasing density they can be quite significant in the edge profile. In order to reduce the errors magnitude the position of the first plasma layer measured with X-mode can be used to help define the non-measured edge profile.

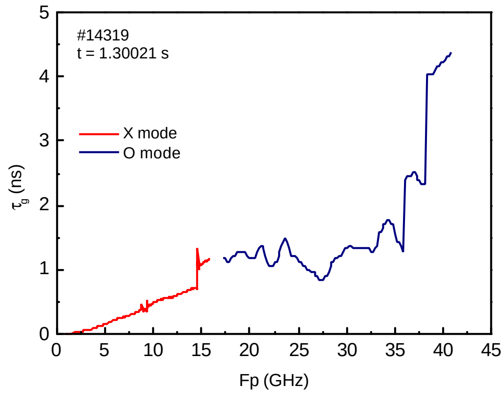

Figure 4.12 – This figure shows the group delay curve obtained using X mode (red) and O mode (blue) data.

4.2.4.4. Tracking of fast plasma events

With the new data processing tools and the ability of reflectometry to perform high resolution measurements, it is possible to track automatically fast profile changes associated with events like ELMs or the L-H transition, and to measure in detail the evolution of important parameters for the edge stability, such as the density pedestal, density gradient and pedestal position and width.

A. Edge pedestal formation across the L to H transition

The algorithm to evaluate automatically the edge pedestal was applied to ASDEX Upgrade high density ($\tilde{n}_e$=1.0×10^{20} m^{-3}) H-mode discharge #14313. Figure 4.13a depicts the D_α signal where a drop can be observed for $t \cong 1.71\,s$ when the L-H transition occurs; the vertical dotted lines indicate the probing time of the first sweep of each burst of eight consecutive measurements performed in 100 μs, spaced by 10 μs.

From the individual profiles shown in Figure 4.13d, measured respectively before and after the transition, as indicated by the arrows in Figure 4.13a, it can be seen that the density shoulder increases abruptly after the L to H transition. The density pedestal starts to form before the transition, during the L phase, coinciding with the onset of the neutral beam power for t=1.45 s. Indeed, the smooth increase of the pedestal density during the L phase and the abrupt jump at the L-H transition can be visualized either from the 2D representation of τ_g or from the pedestal density evaluated automatically

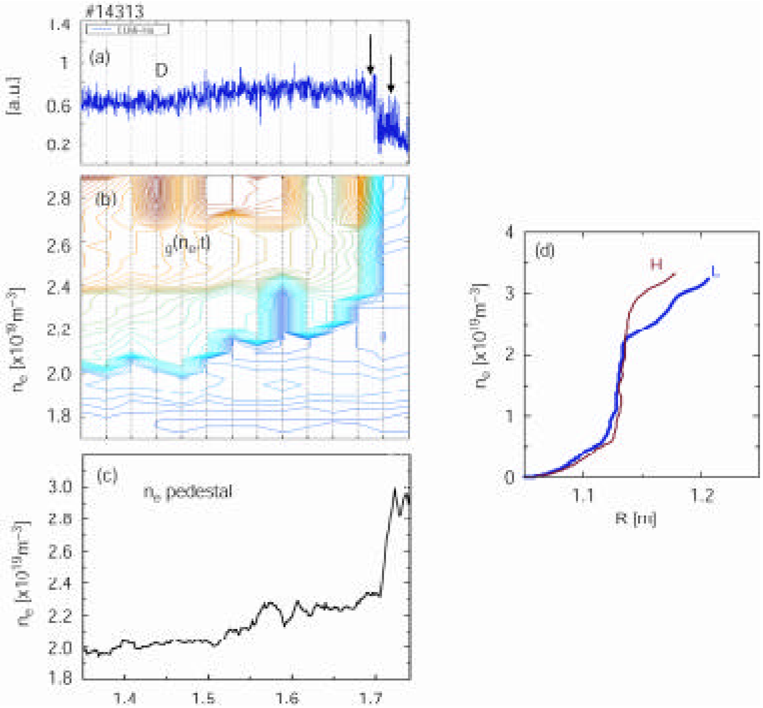

Figure 4.13 – (a) D_α signal displaying a drop at t @ 1.71s, when the L-H transition occurs. The arrows indicate the probing times of the density profiles depicted in (d), showing the abrupt increase of the edge pedestal after the L to H transition. (b) contour plot of group delay versus n_e and time. The bold lines correspond to an overshoot in t_g associated with the sudden change of the profile gradient at the pedestal region. (c) pedestal density, n_{ep}, evaluated automatically from the group delay curve[42]. The temporal evolution of n_{ep} can be visualized either from (b) or (c).

directly from the group delay curve, depicted in Figure 4.13c.

B. Profile evolution during an ELM

Figure 4.14c depicts HFS/LFS density profiles with 20 µs temporal resolution obtained in the ELMy phase of the standard H-mode ASDEX Upgrade shot #14313. Figure 4.14a shows the D_α signal; the vertical lines indicate the corresponding probing times, t_1, t_2 and t_3. The profiles exhibit asymmetric perturbations: higher at the LFS, lower at the HFS. The HFS/LFS measurements can thus be used to study asymmetries in the plasma fluctuations and to extract more accurate density profiles, when plasma turbulence affects less one side than the other (usually the HFS).

Figure 4.14c shows that, at the peak of the ELM (for $t = t_2$), the inner and outer profiles flattens (dot lines) and steepens afterwards (solid lines), moving around a turning point indicated by the arrows in Figure 4.14b. The detailed evolution of the decay lengths corresponding to the density ranges $0.8\text{-}2.0\times10^{19}$ m^{-3} and $2.0\text{-}6.0\times10^{19}$ m^{-3}, depicted in Figure 4.14b, reveal that inside the turning point the profile changes occur in the same time scale of the variations of the D_α signal, while outside no significant modifications are seen. However, after the drop of the D_α radiation the decay length increases significantly indicating an increase of density outside the magnetic separatrix, which may be caused by a reflection from the divertor region.

C. ELM perturbations

Figure 4.15 presents the edge gradient evaluated automatically during the L and ELMy phases of ASDEX Upgrade shot #13165. The radial position of the measurement relative to the separatrix is around -10 cm in the beginning of the L phase decreasing to around -2 cm in the H phase (between ELMs). The density gradient is seen to increase smoothly prior to the L to H and it jumps abruptly for $t \cong 1.22\,s$, when the transition occurs.

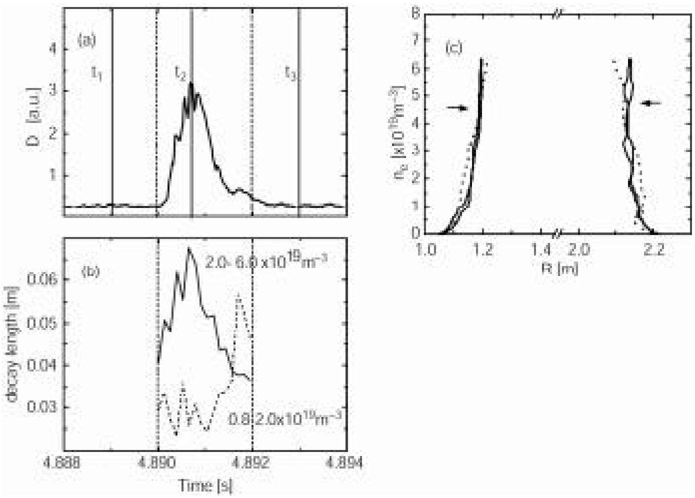

Figure 4.14 – High resolution density profile measurements (20ms), at HFS/LFS obtained in the ELMy phase of H-mode in ASDEX Upgrade high density ($\tilde{n}$=1.0´10^{20}m^{-3}) shot #14313: (a) D_a signal and vertical solid lines indicating the time instants (t_1, t_2 and t_3), where the density profiles in shown in (c) were measured. Profiles flatten at the onset of the ELM (dot lines) and steepens afterwards (solid lines) moving around a turning point, as indicated by the arrows. The profiles exhibit higher perturbations at the LFS than at LHS; (b) temporal evolution of the decay length corresponding to the indicated density ranges during one ELM, obtained automatically from 16 density profile measurements.

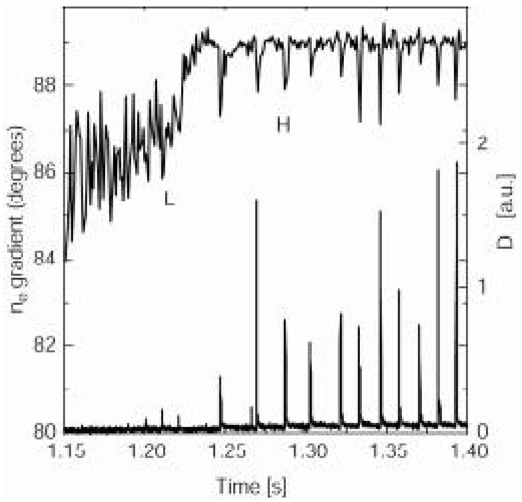

Figure 4.15 – Temporal evolution of the edge gradient across an L-H transition and into the ELMy phase. The radius of the measurement relative to the separatrix is around -10 cm in the beginning of the L phase and -2 cm in the H phase (between ELMs). The smooth increase of the gradient in the L phase and the abrupt jump at the L to H transition (occurring at t~1.22s) are observed in agreement with the results previously shown in Fig.8. During the ELMy phase the edge profile flattens (decrease of the gradient) at each ELM, coinciding with the spikes in the D_a signal.

At each ELM, the edge profile flattens (decrease of the density gradient) coinciding with the spikes in the D_α signal. It can also be noted that the profile perturbations (seen as fast variations of the density gradient), drop as the plasma enters the H-mode regime, in agreement with the expected decrease of plasma turbulence at the plasma edge after the L to H transition.

4.2.5. New applications relevant for ITER[1]

The new applications being investigated are:

- The localization of resonance surfaces aiming at contributing to the estimation of the q-profile, using both experimental data and simulation studies to interpret the complex plasma response;
- The fast evaluation of the plasma position compatible with the requirements of control purposes;
- The estimation of the total magnetic field from O and X mode reflectometry aiming at contributing to the equilibrium reconstruction.

4.2.6. Plasma Physics studies

4.2.6.1. Introduction

The plasma physics studies were focused in the following topics:

- Profiles and fluctuations studies in advanced scenarios;

[1] Described in detail in chapter 8.

- Density profile evolution in improved core confinement with H-mode edge;
- Turbulence reduction during ITB with L-mode type edge;
- HFS/LFS measurements of a quasi-coherent mode at the edge.

4.2.6.2. Profile and fluctuation studies in advanced scenarios

On ASDEX Upgrade the strongest internal transport barriers (ITBs) have been generated through strong heating in the current ramp-up phase in plasmas with L-mode type edge. Transiently the magnetic shear is reversed in the centre and ITBs form mainly in the thermal ion channel. In a second scenario the power (with low values) is increased at the end of the current ramp-up phase, causing a transition into the H-mode. Prior to the L-H transition a weak ITB is formed until the H-mode barrier fully develops and the ITB is extinguished; an enhanced confinement, above standard H-mode is obtained.

4.2.6.3. Density profile evolution in improved core confinement with H-mode edge

In ASDEX Upgrade shot #13037, improved core confinement was achieved with an H-mode edge. Figure 4.16a (upper plot) depicts the time evolution of the average density, neutral beam power PNI, and D_α signal. Density profiles from reflectometry were measured in 20 µs, in bursts of eight consecutive sweeps spaced by 10 µs; the interval between bursts is 45 ms.

Figure 4.16b presents two profiles obtained during the brief ITB phase (at t=1.05 s) and in the H phase (at t=1.5 s). For comparison the density profiles from Thomson scattering diagnostic are shown, in good agreement with the reflectometry results. It should be noted the well defined density pedestals provided by the reflectometry data. The time evolution of the decay length corresponding to the density range 2.52-2.74×10^{19} m^{-3} is shown in Figure 4.16b (lower plot). During the brief ITB phase the decay length decreases significantly, revealing a peaking of the density profile at the foot of the ITB

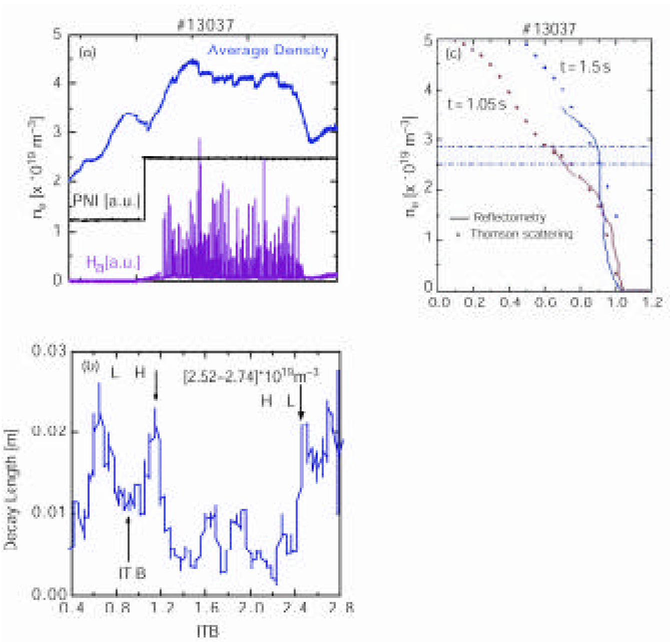

Figure 4.16 – Density profile evolution in a discharge with improved core confinement and H-mode edge. (a) time traces of average density, neutral beam power PNI, D_a signal; (b) decay length corresponding to the density range n_e=2.52-2.74×$10^{19}m^{-3}$; (c) high resolution (20ms) density profiles measured from reflectometry and Thomson scattering diagnostic during ITB (t = 1.05 s) and H phases (t = 1.5 s). During the brief ITB phase the decay length decreases (peaking of density profile); after, it increases as the selected density range, between dash-dot lines in (c), is displaced outwards to the edge until at the L-H transition (t ~1.2 s) the decay length drops abruptly. At the back H to L transition (t ~2.5 s) the lower L-mode density gradient is recovered.

(Figure 4.16c). Afterwards, the decay length increases (following the density increase), while the selected density range is displaced outwards, away from the peaked core region and into the edge, until the L to H transition occurs (at t~1.2 s) and the decay length decreases abruptly (edge profile peaking). At the back (H to L) transition (for t~2.5 s) the decay length increases again abruptly recovering the lower density gradient characteristic of the L phase. In the H-mode phase the increases of the decay length are associated with the flattening of the edge profile during ELMs, which are poorly resolved due to the low sampling rate (45 ms), associated with the burst-mode setup chosen in this particular discharge.

4.2.6.4. Turbulence reduction during ITB with L-mode type edge

A reduction in turbulence has been observed in internal transport barriers (ITB) discharges in ASDEX Upgrade. An example obtained in discharge #13554 is presented in the following, where improved core confinement was achieved with L-mode type edge.

From the temperature profiles for T_i (from charge exchange recombination spectroscopy CXRS) and T_e (from electron cyclotron emission ECE), shown in Figure 4.17b for t≅0.78 s, there is evidence of profile steepening associated with an ITB, stronger in T_i than in T_e, at ρ≅0.45 for t≅0.5-0.62 s (the region probed by reflectometry is between the dashed vertical lines depicted in Figure 4.17b). A stronger steepening is seen both in T_i and T_e at ρ≅0.65 for t≅0.7-0.8 s. Reflectometry measurements were performed with several reflectometry channels operating in fixed frequency with a sampling rate of 500 kHz during 6.2 s.

Figure 4.18 shows the results from the 43 GHz channel, probing the density layer $n_e = 2.3\times10^{19} m^{-3}$, obtained in a similar discharge (#13353): (a) the spectrogram of the reflected signal showing the time resolved spectrum of the plasma fluctuations at the reflecting region, and (b) the integrated power of the fluctuations between 1 kHz and 250 kHz.

When reflection starts ($t \cong 0.3\,s$), the power increases as the density rises, while the cut-off layer moves outward (the positions of the reflecting layers are inferred from the density profiles measured with Thomson scattering diagnostic). Two reductions of the high frequency part of the spectrum are observed starting at t≅0.55 s t ~0.55 and t≅0.55 s, when the cut-off layer is located at the foot of the ITB, for ρ≅0.5 and ρ≅0.65, respectively. A small power decrease is seen (≤ 3 dB) when the ITB is weak and a strongest decrease (> 10 dB) is found when the ITB is stronger. From the analysis of the density profiles no significant change of gradient occurs in the probed region during ITB and therefore the observed drops should be due to a decrease of the level of fluctuations. The suppression of turbulence seems to be associated with the $E\times B$ shearing stabilization of turbulence. After the ITB, the density continues to rise and the level of fluctuations attains values higher than before the ITB. The two drops of the fluctuation level are correlated both spatially and temporally with the ITBs, illustrating the high sensitivity of reflectometry to changes in the level of turbulence and the high spatial and temporal resolution of the core measurements.

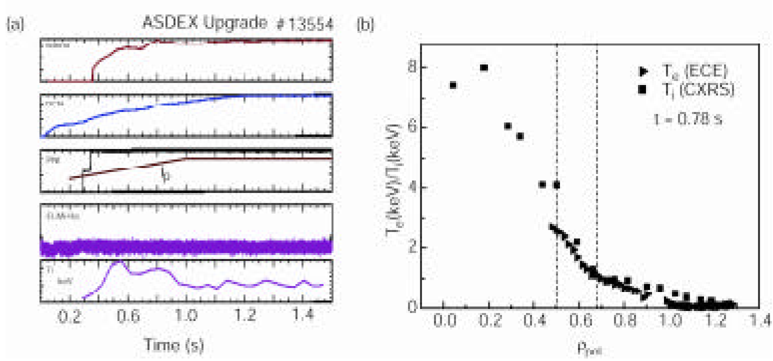

Figure 4.17 – Time traces of relevant parameters in ASDEX Upgrade discharge #13554, with improved core confinement and L type plasma edge. (a) stored energy Wmhd, average density DCN, NBI power, plasma current Ip, D_a signal, and central ion T_i. (b) T_i and T_e profiles, from ECE and CXRS diagnostics, with evidence of profile steepening associated with an ITB, around r ~0.65. The region probed by reflectometry is within the dashed lines.

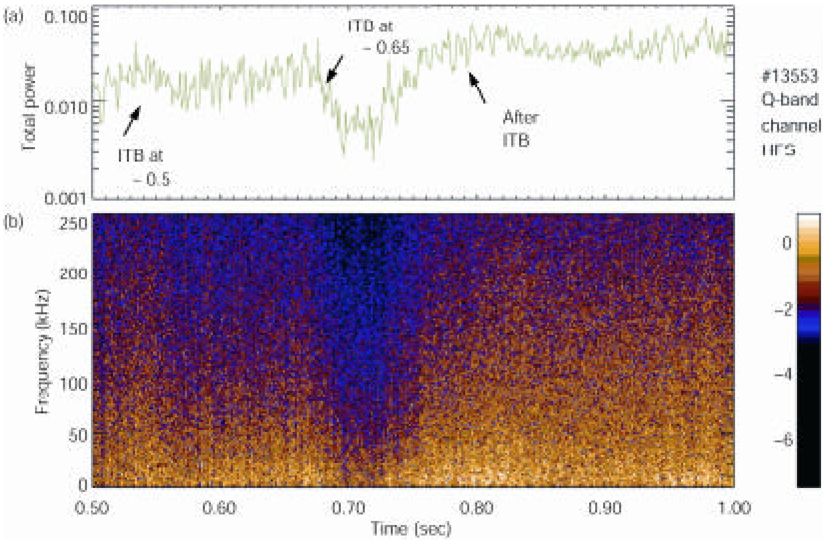

Figure 4.18 – (a) spectrogram of the reflected signal from the 43 GHz channel probing density layers $n_e=2.3\times10^{19}m^{-3}$; (b) integrated power of the fluctuations between 1 kHz and 250 kHz. Two reductions of the high frequency part of the fluctuation spectrum are observed at t ~ 0.55 s and for t: 0.7 - 0.82 s, when the cut-off layer is located at the foot of the ITB. The strongest decrease is observed when the ITB is stronger for t: 0.7 - 0.82 s.

The above results demonstrate the capability of reflectometry to make detailed measurements in the narrow regions where the external and internal barrier are formed, and the importance of profile measurements to locate the reflecting layers where fluctuations are measured, to take account of profile variations that occur along the discharge.

4.2.6.5. HFS/LFS measurements of a quasi-coherent mode at the edge

To check for similarities between the type-II ELMy H-mode in ASDEX Upgrade (AUG) and the ELM free enhanced D-Alpha (EDA) mode in ALCATOR C-Mod we investigated on AUG the edge fluctuations using reflectometry. In ALCATOR C-Mod a quasi-coherent mode is observed in the edge, with typical frequencies around 100 kHz, which may be responsible for particle transport through the edge barrier. In contrast no enhancements in fluctuations are observed around 100 kHz in AUG in regimes with favorable type-II ELMs (at high heating levels), but this feature could be seen in "classical" H-modes with type-I and type-III ELMs and reduced heating.

The enhanced fluctuations on AUG have been, so far, only detected by reflectometry. An example obtained in shot #13473 is shown in Figure 4.19. The enhanced fluctuations are detected in the 49 GHz reflectometry channel, when the L to H transition occurs and are present during type I and type III ELMs and in ELM free phases. When the NI power is increased this feature vanishes re-appearing when the power is reduced from 5 MW to 2.5 MW. The phase perturbation seen by reflectometry is sensitive to the density gradient according to (in the long fluctuation wavelength limit)

$$\tilde{\varphi} = 4\pi/(c/F)(\tilde{n}/n)L_n^{-1},$$

where F is the probing frequency and L_n is the density scale length at the cutoff density. It is, therefore, important to determine if the observed changes in fluctuations are not due to density gradient variations.

The density profiles are presented in Figure 4.19c, indicating that the density layers probed with the 49 GHz channel (see arrows), are situated at radial positions relative to the separatrix between 0 and 1 cm. They reveal that the position and gradient at cut-off region does not change when the NI power is increased from 2.5 MW to 5 MW, thereby confirming that the mode disappears due to the increase of the heating power. This shows the importance of profile measurements for the interpretation of fluctuations measurements.

In order to study the radial profile of fluctuations, measurements were performed in a similar shot (#14330) with six reflectometry channels operating in fixed frequency. In the time resolved frequency spectra of the reflected signals (Figure 4.20) an

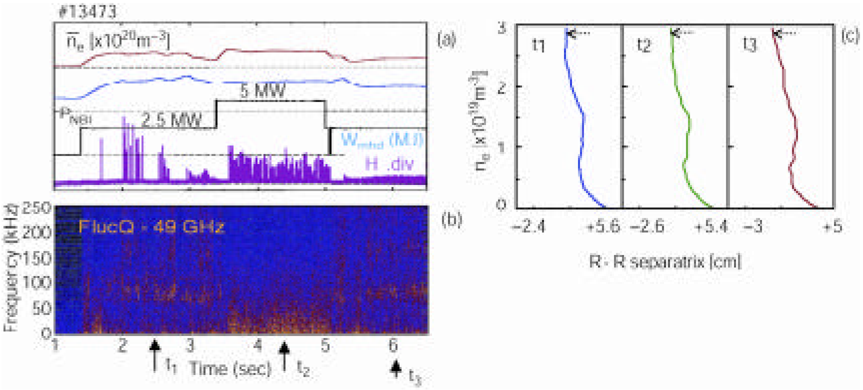

Figure 4.19 - Study of enhanced fluctuations that may play an important role on transport across the edge barrier. (a) time traces of $\tilde{n}_e$, stored energy W_{mhd}, NI power and H_α signal at the divertor, and (b) the time resolved frequency spectrum of the 49 GHz reflectometry channel, probing edge layer n_e : 2.6 x10^{19} m^{-3}. Edge fluctuations (~100 kHz) are observed with reflectometry that vanishes when NI power is increased, appearing again when the power is reduced. Density profiles (c) do not change significantly at the probed density layers (indicated by the arrows), showing that this effect should be due to the NI power changes.

higher level of fluctuations is observed at the channels probing the highest density layers (n_e=2.6x10^{19} m^{-3}). The level of fluctuations is stronger at the LFS suggesting that the mode may be more concentrated on the outer side of the plasma.

In view of the above results, dedicated experiments are foreseen to measure the radial profile of the fluctuation level (inner and outer) using all the HFS/LFS reflectometry channels to determine the characteristics of the mode (ballooning or peeling type). 2D simulations featuring the antenna characteristics of each channel are under way to support a quantitative interpretation of the experimental results.

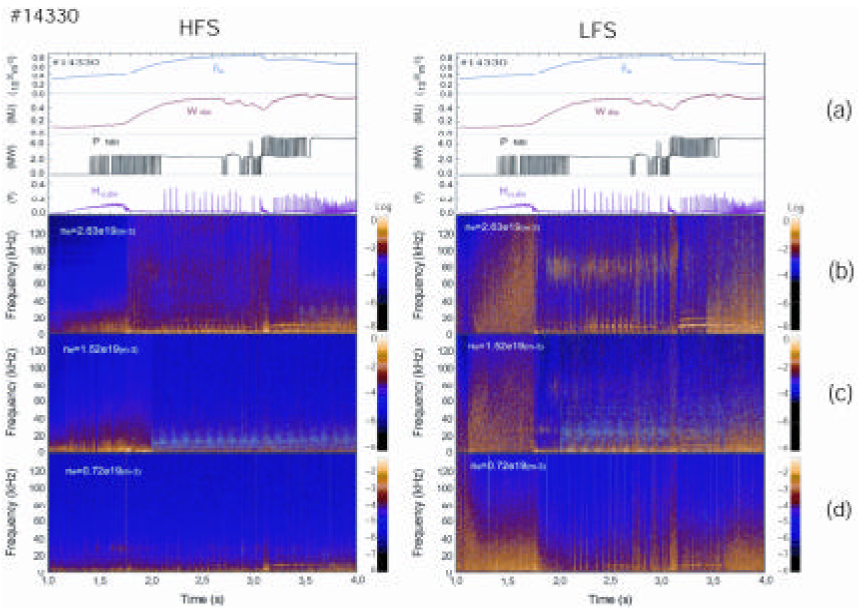

Figure 4.20 – Estimation of radial profile of edge fluctuations with 6 reflectometry channels (at fixed frequencies). In (a) it is shown time traces of $\tilde{n}_e$, stored energy W_{mhd}, NI power and H_α signal at the divertor. (b), (c) and (d) display time frequency resolved spectra of signals reflected from density layers n_e : 0.72x10^{19} m^{-3}, 1.52x10^{19} m^{-3} and 2.63x10^{19} m^{-3}, at HFS/LFS.

4.3. MHD AND TURBULENCE

4.3.1. Introduction

Activities on MHD and Turbulence have been focussed on:

- Studies of disruptive events
- Turbulence studies in the edge/SOL region

4.3.2. Studies of disruptive events at ASDEX Upgrade

The following main activities were carried out:

- Elaboration of a proposal to study disruptive events at ASDEX Upgrade, in order namely to extend the studies carried out at FOM (in RTP tokamak) to larger ITER-like tokamaks.
- Beginning of the work aiming at (i) studying fast plasma events (modifications of T_e, n_e) during the energy quench of ASDEX Upgrade major disruptions; (ii) analysing possible amelioration of ASDEX Upgrade, with ECRH; and (iii) investigating the fast particle dynamics on the presence of internal relaxations (sawteeth) and disruptive instabilities.

4.3.3. Turbulence studies in the edge/SOL region

The following main task was made:

- Definition of a working plan, which is focussed on the topic of turbulence studies in the edge/SOL regions of the ASDEX Upgrade plasma. It involves work on an existing numerical code for driftwave turbulence modelling, in order to extend it, namely by introducing the effects of neutrals recycling at the divertor plates.